Harmonic Components and Dispersion of Mobile Network Signals due to Fiber-Optical Transmission

Attila HILT, Eszter UDVARY, Gábor JÁRÓ, Tibor BERCELI

Abstract **– Several system applications require optical transmission of very high bit-rate digital as well as microwave and millimeter-wave carrier signals. Without completeness, a few recent applications are mentioned such as: 5G and Radio-over-Fiber (RoF) systems, Gigabit Passive Optical Networks (GPON), optical interconnection within Cloud for telecommunication Network Elements (NE), upgrade of mobile access, backhaul and core networks (NW) or phased array and antenna beamforming applications. Both chromatic dispersion and harmonic distortion result in unwanted limitations in the maximum distance and bandwidth. Dispersion penalty has been widely investigated in fiber-optical links transmitting microwave or millimeter-wave signals. However, less attention is addressed to the effect of the harmonics of the modulating fundamental electrical signal. This paper presents some theoretical and experimental results estimating the level of harmonics during the optical transmission.**

Index Terms **– microwaves, Radio-over-Fiber, 5G, optical transmission, single-mode fiber, harmonics**

I. Introduction

Transmission of radio-frequency (RF) signals over optical fiber gained significant interest in the last decades [1-9]. Several new perspective applications like 5G and Radio-over-Fiber networks or Cloud for telecommunications ("telco-cloud") require wideband optical links applying either laser diodes (LD) or external modulators (Fig.1).

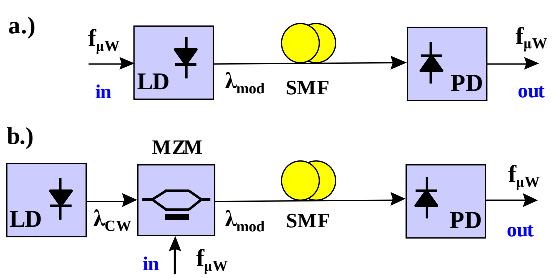

Fig.1. Optical modulation with µW frequency
a.) direct by LD and b.) external by MZM.

When using standard single-mode optical fiber (SMF) at λ=1550 nm wavelength for such wideband transmission systems (Fig.1), chromatic dispersion (CD) of the optical fiber becomes one major limiting factor. At the output of the optical system, undesired harmonics appear beside the wanted signal, in case of both λ=1300 nm and λ=1550 nm.

Several factors contribute to the undesired harmonics. The nonlinearities of the electrical-to-optical (E/O) and the optical-to-electrical (O/E) conversions, signal impurity at the fiber input, dispersion in the optical transmission and coherent beating in the photodetection at the fiber end.
In our paper the fiber length-bandwidth product is investigated for optical transmission over SMF. In the next part, mobile application examples are shown. In the third part transmission and harmonic measurement setups are shown. In the fourth part, we present a numerical model. It is shown that the second harmonic of the modulating electrical signal is always generated in intensity modulated - direct detection links (IM-DD). In the fifth part of the paper the different electrode variants of the optical modulator and the effect of the modulator bias settings are discussed. It is shown that modulator chirp can reduce the undesired effect of fiber dispersion. The presence of harmonic signals is verified up to the near-mmW range experimentally in the last part of the paper.

II. Mobile Applications: 5G, Radio and Core Cloud, Radio Remote Head

Fiber-optic techniques have been widely used in the legacy transmission and transport systems of mobile networks e.g. in backbone. Recently more and more new areas demand extra wide bandwidth what optical fibers can ensure. These applications are 5G, carrier distribution in next generation mobile systems, radio and core networks cloudification and interconnections in the converged core (Fig.2).

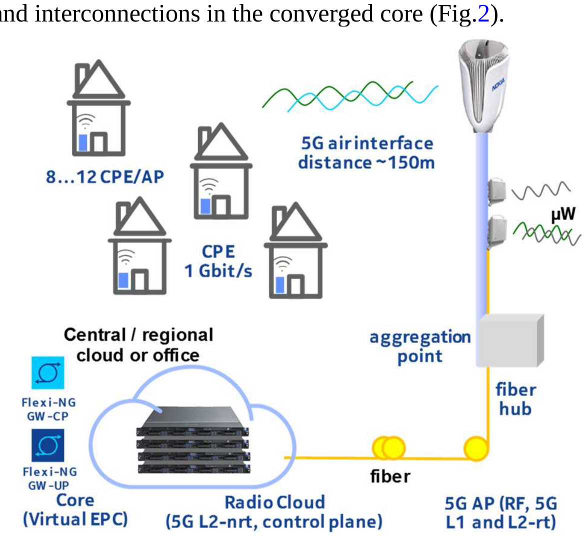

Fig.2. 5G access and radio cloudification

5G targets 10 Gbit/s peak user rates, 2 GHz bandwidth and latencies of less than 1 ms. The recommended carrier frequencies for future 5G systems are falling into the microwave (µW) and millimeter-wave (mmW) ranges of

Paper submitted: 12 April 2017.
Attila Hilt and Gábor Járó are with Nokia Mobile Networks, Cloud Core, Skypark office, H-1082 Budapest, Bókay János u. 36-42, Hungary (e-mails: attila.hilt@nokia.com, gabor.jaro@nokia.com).
Eszter Udvary and Tibor Berceli are with BME, Budapest University of Technology and Economics, Hungary, Department of Broadband Infocommunications and Electromagnetic Theory, H-1111 Budapest, Egry József u. 18. (e-mails: udvary@hvt.bme.hu, berceli@hvt.bme.hu).

3-5 GHz, 26-39 GHz. But 5G carrier frequencies even up to 86 GHz are considered.

Another example of the efficient use of fiber-optics is due to the increased capacity demand in mobile backhaul for Single Radio Access Network (SRAN). SRAN allows mobile NW operators to support multiple communications standards for wireless services (2G, EDGE, 3G, HSPA, LTE, WiFi etc.) over a common network infrastructure in a flexible way. Single RAN technology is designed to support a multitude of sharing options like baseband, RF, mobile backhaul, transport, RF spectrum and common embedded O&M. The consolidated hardware (HW) and software (SW) incorporate e.g. software-radio, multiband and Multiple-Input Multiple-Output (MIMO) antenna solutions. In the mobile backhaul part legacy access microwave links cannot fulfill any more the significantly increased capacity demands of cell sites. The high frequency fees for the wider RF bandwidth allocations makes fiber installation or lease costs in longer term competitive. In dense urban areas, several other factors also limit the installation of new µW/mmW links: parabolic antennas cannot be installed on rooftop of historical buildings, there are latency and interference limits. As shown in Fig.3 fiber-optical chaining of remote radio heads (RRH) may provide solution for such scenarios.

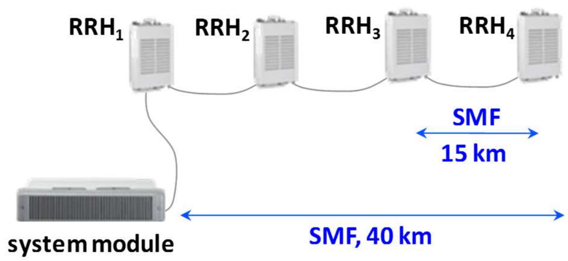

Fig.3. Optical chaining of Remote Radio Heads

III. Transmission of Wideband Signals over Single-Mode Optical Fiber

The optical transmission of high-speed (Gigabit/s) digital signals as well as µW or millimeter-wave analogue signals (e.g. for 5G carrier distribution) is significantly limited. The main limiting factors are fiber dispersion and harmonic distortion. Chromatic dispersion can be measured with an electrical network analyzer that is extended into the optical domain, as shown in Fig.4. Usually, a very short reference optical cable is used for calibration. Fig.5 shows measured transmission curve as a function of the intensity modulation (IM) frequency. As seen, the penalty in the optically transmitted analogue RF signal is crucial due to CD. The plot belongs to an optical SMF length of L=60 km. Sharp transmission zeros are visible around 7.68, 13.46 and 17.58 GHz frequencies. As seen in Fig.5, the rejections of the optically transmitted signal are more frequent at higher frequencies. The frequencies of the transmission zeros are depending on the fiber length L that makes system design even more difficult. To our best knowledge, the effect of chromatic dispersion has been published and experimentally demonstrated first in [8, 10-11]. Several different methods have been proposed to overcome the mentioned drawback of dispersion [12-21, 25-27].

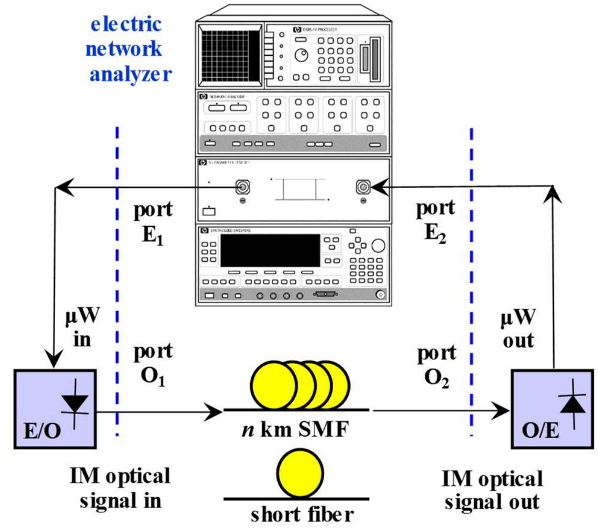

Fig.4. Fiber transmission measurement with an electrical network analyzer extended to the optical domain

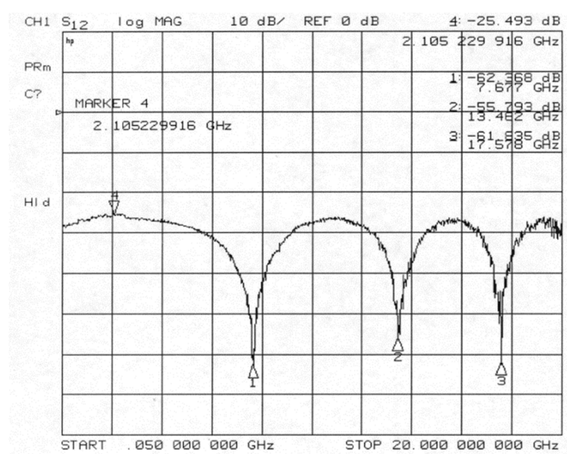

Fig.5. Measured dispersion penalty as a function of µW frequency (intensity modulation, L = 60 km fiber).

The test setup for harmonic distortion measurements is shown in Fig.6. On the transmitter side a laboratory microwave signal source is driving the E/O converter (HP83420A Lightwave Test Set, λ=1300 nm). At the reception side a microwave spectrum analyzer (HP8562A) is connected to the output of the wideband photodetector.

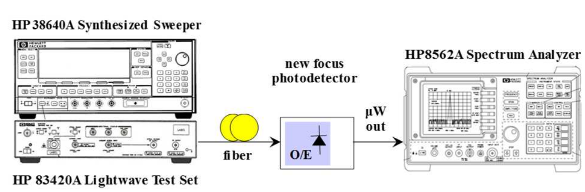

Fig.6. Detected 2nd and 3rd harmonics (260…990 MHz) of an optically transmitted RF signal (swept in 130-330 MHz).

The detected harmonic components of the optically transmitted RF signal are shown in Fig.7. The fundamental signal was swept in the f_{RF}=130-330 MHz range. Strong second and third harmonics are visible in the 260-660 MHz and 390-990 MHz ranges, as it was detected by the wideband photoreceiver and spectrum analyzer.

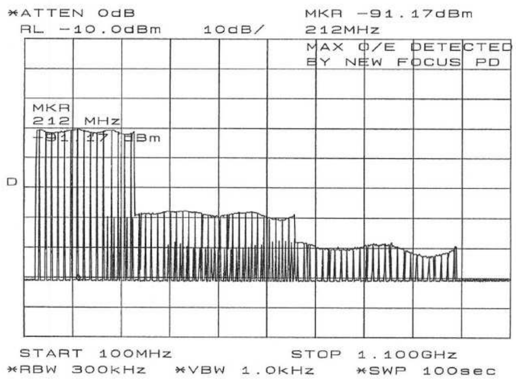

Fig.7. Detected 2nd and 3rd harmonics (260…990 MHz) of an optically transmitted RF signal (swept in 130-330 MHz).

IV. Numerical Model of Harmonics and Dispersion in Optical Transmission

The output optical spectra of both direct modulated laser diodes and external optical intensity modulators contain sideband peaks around the optical carrier [10, 15, 19-28]. At very high IM frequencies falling into the μW/mmW range, these sideband peaks have a frequency separation in the order of 10 GHz or even beyond. These spectral components propagate with different speed in the optical fiber due to chromatic dispersion [10, 24, 27]. The typical dispersion value of standard SMF is about D=17 ps/nm/km around λ=1550 nm wavelength. As a result, depending on the fiber length L and the IM frequency f_{RF}, a complete rejection of the modulation content can happen. The power P_{RF} of the electrical signal detected at the PD is given as [8, 11, 12, 20, 27]:

$$P_{RF}^{[dB]} \propto 20\log\left|\cos\left(cD\pi L\left(f_{RF}/f_{opt}\right)^2\right)\right|. \qquad \text{Eq.1.}$$

In the simple analysis, only three spectral lines are considered in the optical field of E(ω) at the SMF input. This approximation significantly reduces the calculation difficulty, so it is possible to derive the result of Eq.1 analytically. In the general case, however the optical field is composed of several spectral at the fiber input (Fig.8).

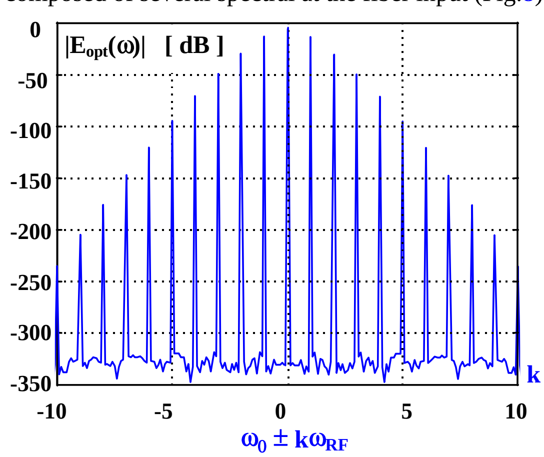

Fig.8. MZM output field: DC bias for linear operation, $\gamma = V_{DC}/V_\pi = 0.5$, $\alpha = V_{RF}/V_\pi = 0.4$.

At the detection side the amplitude and phase of the optical field spectral components are determined by the optical transmitter (LD or external modulator) as well as by the parameters of propagation in the dispersive fiber [27]. In this part, based on the coherent model of the μW optical link, we simulate the effect of chromatic dispersion in the general case of several spectral lines. Fig.8 shows the amplitude of the optical field, calculated at the output of the Mach-Zehnder Modulator (MZM) that is biased for linear operation (also called as quadrature bias, see Fig.9). In the coherent model the calculation is based on the optical field E_{opt} and not on the optical intensity I_{opt}. Coherent models can properly explain the presence of different harmonics of the μW modulation signal.

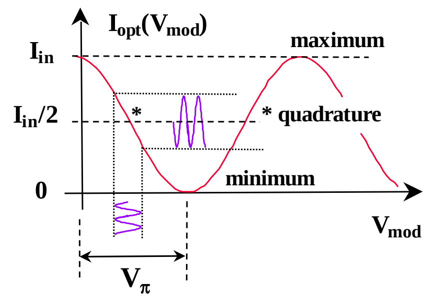

Fig.9. Transmittance and bias of the Mach-Zehnder Modulator.

Fig.10 presents simulation results of harmonic evolution in the dispersive optical transmission based on the optical field of Fig.8, which is launched into the fiber. As seen in Fig.10, also second harmonic and higher order harmonics are generated due to propagation in the dispersive fiber. (Fiber, modulator and photodetection losses are neglected by normalization.) According to the measurements of Fig.4 - Fig.7, the transmission is distorted by harmonics and rejections at specific modulation frequencies.

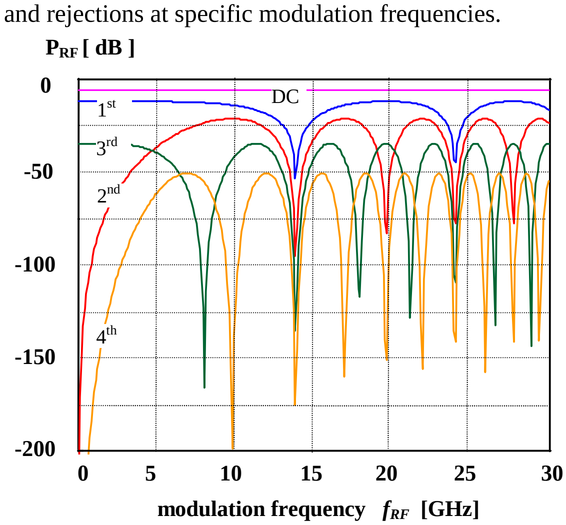

Fig.10. Detected signals after propagation in dispersive fiber of L=19.2 km, input optical field as Fig.8.

When the MZM is biased for linear operation (quadrature point in Fig.9), there are only odd components present in the optical intensity [20]. However, in the optical field both even and odd spectral components are present (Fig.8). When this optical field is launched into a SMF, due to chromatic dispersion even intensity components will appear after propagation. Calculated levels of harmonic signals are shown in Fig.10. Since the phase of the harmonics are rotated faster in the fiber than phase of the fundamental signal, the second harmonic has two times, the third harmonic has three times more rejections between two rejections of the fundamental. As mentioned, this phenomenon cannot be explained by the incoherent models of the µW optical link [8, 10-27].

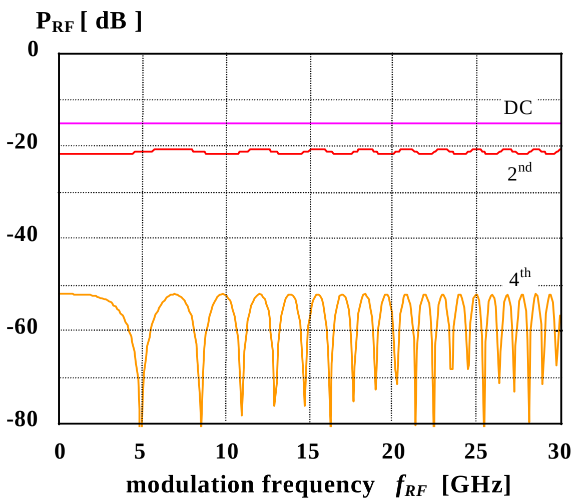

Fig.11. Detected RF signals after propagation in dispersive fiber of L=19.2 km, input field as Fig.12.

When the MZM is biased for minimum transmission (V_π in Fig.9), the second harmonic of the modulation signal will not be rejected, even after propagation in a several km long dispersive fiber (Fig.11). The reason of this phenomenon is the coherent beating at the photodetector, as explained in [21-24]. In this case the phase differences cannot create complete rejection, since the optical carrier is suppressed as shown in Fig.12.

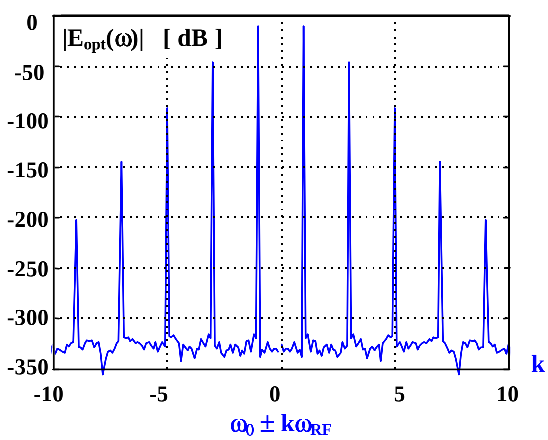

Fig.12 MZM output optical field at DC bias for minimum transmission, $\gamma = V_{DC}/V_\pi = 1$, $\alpha = V_{RF}/V_\pi = 0.4$.

As an advantage of the suppressed carrier optical modulation (SCOM), only the subharmonic of the desired µW/mmW signal is required to drive the optical modulator. This method can be used for RF frequency doubling [11]. Based on the idea presented in Fig.8-12 different optical methods are investigated to overcome the chromatic dispersion effect. Dual mode laser diode [16], self-heterodyning technique [17], and optical single sideband (OSSB) modulation are proposed. These solutions are described in the literature in details [11-27].

V. Effects of Optical Modulator Types and Bias Settings

The model discussed above is quite general: the simulation method is suitable for calculating the simultaneous effects of fiber dispersion, modulator bias [29, 30] in external modulation or chirp (also known as Henry-factor) of direct modulated laser diodes [19-26]. The push-pull MZM [31-33] and its possible cross sections are shown in Fig.13.

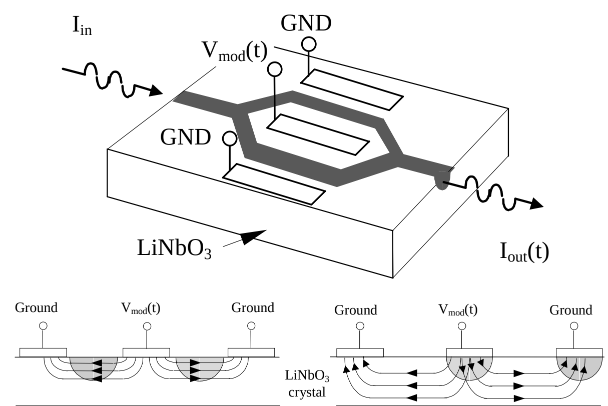

Fig.13. Push-pull MZM. Possible cross sections of push-pull MZ modulators having symmetric CPW electrodes.

Surface plot of Fig.14 presents the calculated level of the detected signal at fundamental frequency, as a function of fiber length L and modulation frequency f_{RF}.

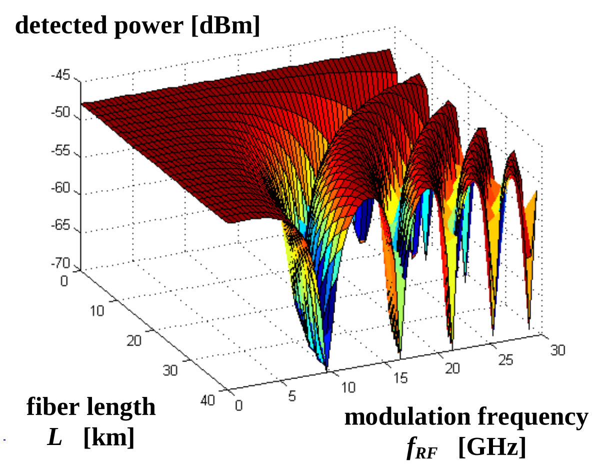

Fig.14. Detected power level of µW signal transmitted optically in dispersive fiber. Linear modulator bias of γ =0.5, α =0.25, D=17ps/km/nm, photodiode responsivity: R_{PD}=0.35 A/W.

The voltage on the MZM can be written as:

$$V_{mod}(t) = V_{DC} + V_{RF}(t) \qquad \text{Eq.2.}$$

where V_{DC} is the bias voltage and $V_{RF}(t)$ is the modulation signal. As seen in Fig.9, the V_{DC} bias voltage drives the modulator to its linear (called as quadrature) or to its minimum transmission (so called half wave voltage:

$V_{DC} = V_\pi$) point. The normalized modulator bias voltages are denoted as:

$$\gamma = V_{DC}/V_\pi \qquad \text{Eq.3.}$$

$$\alpha = V_{RF}/V_\pi. \qquad \text{Eq.4.}$$

and they are introduced for calculation simplicity in the simulation program [24]. Compared to the fiber penalty plot of Fig.10 now the losses due to optical modulation as well as detection have been introduced in the model. For better visibility, the linear fiber loss is neglected in Fig.14.

In Fig.15 asymmetric co-planar electrode configuration is shown. As seen in the left cross section, unbalanced operation is possible in this case too. The difference compared to the previous push-pull MZM electrode configuration results in a higher level of modulator chirp. The "single-arm" MZM gives different output optical field than that of the push-pull MZM (presented in Fig.13).

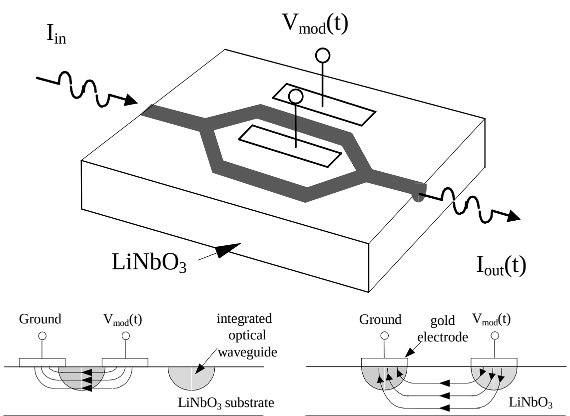

Fig.15. Asymmetric CPW electrode MZM and its possible cross sections: unbalanced and push-pull operation.

Fig.16 plots again the calculated power level of the μW signal detected at the fundamental frequency as a function of modulation frequency f_{RF} and fiber length L. Compared to Fig.14, now the frequency of the first rejection is a bit increased in Fig.16 and a slight overshoot can be seen before it. It is due to the combined effect of modulator chirp and fiber dispersion [25, 26, 28].

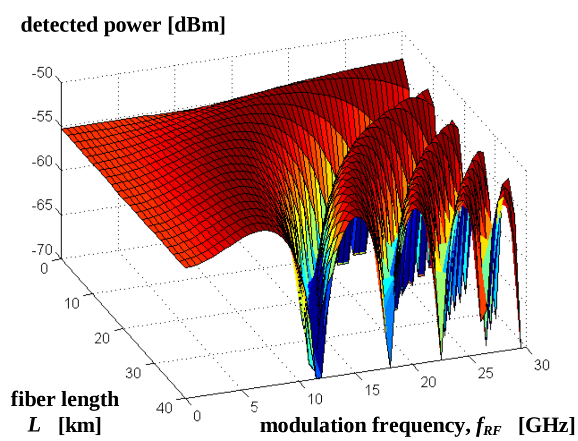

Fig.16. Dispersion compensation by the chirp of the unbalanced (one arm modulated) MZM.

VI. Experimental Results

Fig.17 shows the photograph of the experimental setup. The electrical and the lightwave sources, as well as the optical modulator were HP laboratory instruments: HP83422A Lightwave Modulator, HP83424A Lightwave CW Source, HP11982A Lightwave Converter. All the HP instruments were connected to the controlling computer over Hewlett-Packard Interface Bus (HP-IB). The optical CW source was set to launch λ=1550 nm wavelength. The frequency of the electrical signal source f_{RF}, which modulated the optical transmitter, and the center frequency of the spectrum analyzer have been set simultaneously by the measurement control and data acquisition software (HP VEE). First the spectrum analyzer measured the level of the detected fundamental signal, then its 2nd and 3rd harmonics. The spectrum analyzer used the 'peak search' function to find the signal peak of the measured harmonic near the center frequency, that was programmed by the controlling computer via HP-IP.

Fig.17. Photograph of the experimental setup for the fundamental RF level measurements

First the optical transmission was calibrated by inserting a short optical fiber between the optical modulator and the photodetector. Fig.18 refers to the calibration with a short patch cord. Then the detected levels of the fundamental, second and third harmonic signals have been measured by the computer controlled spectrum analyzer.

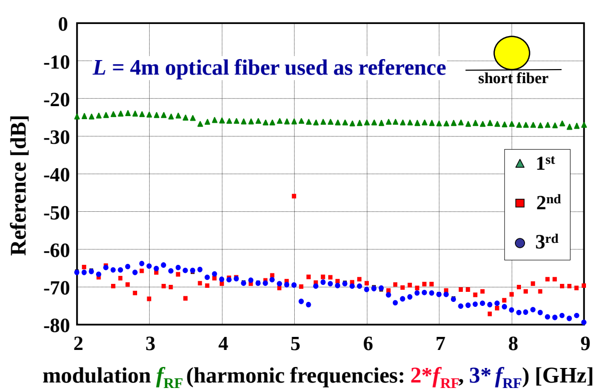

Fig.18 Calibration with a short optical fiber.

Different single-mode fiber lengths of L = 30, 40, 50 and 60 km have been measured. The measured results are normalized to the calibration. This way the frequency dependent E/O and O/E conversion losses have been removed from the results plotted. Fig.19 shows the measured transmission for the fundamental signal f_{RF}. The frequency was swept in the range of f_{RF}=2-9 GHz.

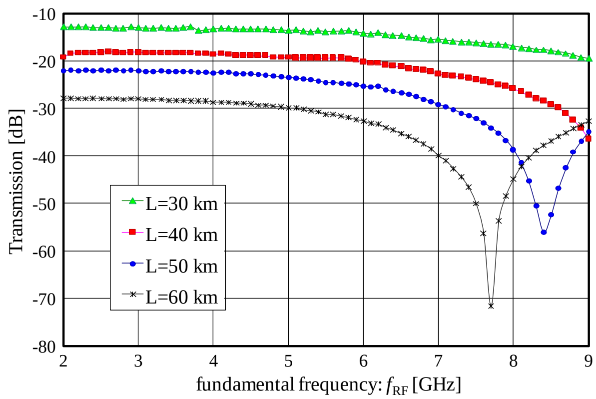

Fig.19. Measured transmission for the fundamental signal: f_{RF}.

Fig.20 shows the 2nd harmonic in the range of $2 \cdot f_{RF}$=4-18 GHz. Finally, Fig.21 plots the 3rd harmonic in the frequency range of $3 \cdot f_{RF}$=6…26.5 GHz (the upper band edge was limited by the frequency range of the spectrum analyzer). As the fundamental signal, the harmonics also exhibit minima and maxima. The exact frequencies of the measured minima and maxima are depending on the fiber length L, as it is expected from the numerical model. The transmission zeros are more frequent at higher frequencies.

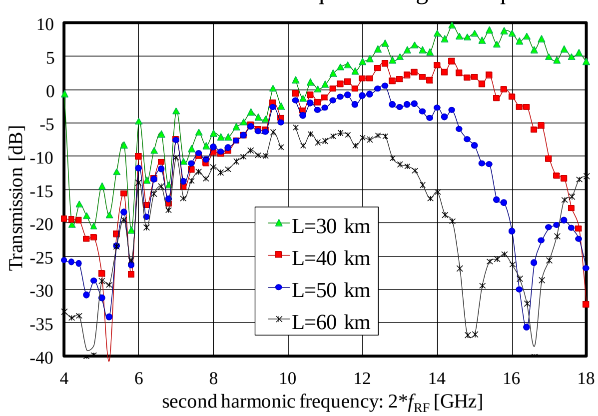

Fig.20. Measured transmission for the 2nd harmonic: $2 \cdot f_{RF}$.

Conclusions

The demand for transmitting broadband data and high frequency carrier signals is continuously increasing due to several new applications such as 5G, RoF, SRAN, GPON, telco-cloud or antenna beamforming. In this paper the fiber-optical transmission of µW and mmW signals have been discussed. The undesired effects of harmonic distortion and chromatic dispersion have been investigated. The generation of second and higher order harmonics of the modulation signal in the optical path has been verified both theoretically and experimentally. We presented a general model to calculate harmonic levels and the effect of chromatic dispersion numerically. Levels of detected harmonics are estimated by the developed coherent model. Experimental examples have shown clearly the presence and evolution of harmonics in the µW photonic link. It was shown, that similarly to the fundamental signal, the harmonics also exhibit minima and maxima due to propagation in dispersive fiber. It was shown that they considerably influence the maximum available bandwidth and fiber length.

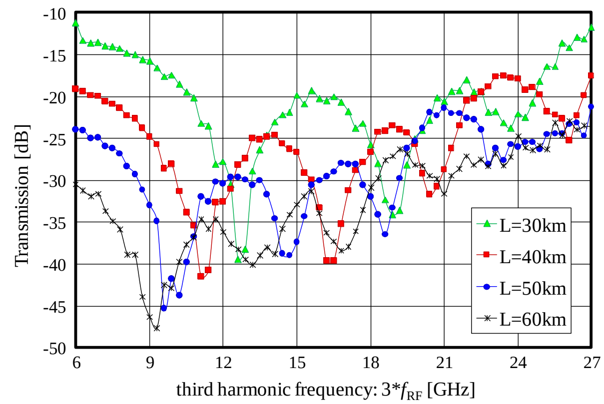

Fig.21. Measured transmission for the 3rd harmonic: $3 \cdot f_{RF}$.

Acknowledgments

The authors wish to thank Prof. Dr. István Frigyes, Dr. Tamás Marozsák and Dr. Ghislaine Maury for the fruitful discussions. Support of the French-Hungarian co-operation *'Balaton'* as well as *FiWiN5G, Fiber-Wireless Integrated Networks for 5th Generation delivery*, a Marie Skłodowska-Curie Innovative Training Network is acknowledged.

References

[1] ITU-T Series G: "Transmission Systems and Media, Digital Systems and Networks, Radio-over-fibre (RoF) technologies and their applications, Supplement 55", July 2015.

[2] Rec. ITU-R F.1332-1: "Radio-Frequency Signal Transport through Optical Fibres", The ITU Radiocommunication Assembly, May 1999.

[3] Stavros Iezekiel, editor: "Microwave Photonics: Devices and Applications", *John Wiley & Sons, Ltd.*, 2009.

[4] Chi H.Lee, editor: "Microwave Photonics", *2nd edition, CRC Press, Taylor & Francis Group*, 2013.

[5] Hamed Al-Raweshidi, Shozo Komaki editors: "Radio over Fiber Technologies for Mobile Communications Networks", *Artech House*, Boston, London, UK, 2002.

[6] Anne Vilcot, Béatrice Cabon, Jean Chazelas: "Microwave Photonics, From Components to Applications and Systems", *Kluwer Academic Publishers*, 2003.

[7] János Ladvánszky: "Circuit theoretical aspects of optical communication links", *17th International Conference on Transparent Optical Networks, ICTON'2015, paper Tu.B6.1*, Budapest, Hungary, July 2015.

[8] Wim van Etten, Jan van der Plaats: "Fundamentals of Optical Fiber Communications", *pp.62-68, Prentice Hall Int. Series in Optoelectronics*, UK, 1991.

[9] János Ladvánszky: "Frequency Invariance in a New Allocation Scheme for Optical Communications", *ICTON'2016*, Trento, Italy, 10-14 July 2016.

[10] Roger W.Wong, Paul R.Hernday, Daniel R.Harkins: "High-speed Lightwave Component Analysis to 20 GHz", *Hewlett Packard Journal, pp.6-13*, February 1991.

[11] Harald Schmuck: "Comparison of optical millimetre-wave system concepts with regard to chromatic dispersion",

Electronics Letters, Vol.31, No.21, pp.1848-1849, 12^{th} Oct. 1995.

[12] U.Gliese, S.Nørskov, T.N.Nielsen: “Chromatic Dispersion in Fiber-Optic Microwave and Millimeter-Wave Links”, *MTT, Vol.44, No.10, pp.1716-1724,* October 1996.

[13] J.Park, W.V.Sorin, K.Y.Lau: “Elimination of the Fibre Chromatic Dispersion Penalty on 1550 nm Millimetre-Wave Optical Transmission”, *Electronics Letters, Vol.33, No.6, pp.512-513,* 13^{th} March 1997.

[14] Graham H.Smith, Dalma Novak, Zaheer Ahmed: “Overcoming Chromatic-Dispersion Effects in Fiber-Wireless Systems Incorporating External Modulators”, *MTT, Vol.45, No.8, Part II, pp.1410-1415,* August 1997.

[15] Graham H.Smith, Dalma Novak: “Broad-Band Millimeter-Wave (38 GHz) Fiber-Wireless Transmission System Using Electrical and Optical SSB Modulation to Overcome Dispersion Effects”, *IEEE PTL, Vol.10, No.1, pp.141-143,* January 1998.

[16] David Wake, Claudio R.Lima, Phillip A.Davies: “Optical Generation of Millimeter-Wave Signals for Fiber-Radio Systems Using a Dual-Mode DFB Semiconductor Laser”, *MTT, Vol.43, No.9, pp.2270-2276,* September 1995.

[17] Rolf Hofstetter, Harald Schmuck, Rolf Heidemann: “Dispersion Effects in Optical Millimeter-Wave Systems Using Self-Heterodyne Method for Transport and Generation”, *MTT, Vol.43, No.9, pp.2263-2269,* September 1995.

[18] Attila Hilt, Attila Zólomy, Tibor Berceli, Gábor Járó, Eszter Udvary: “Millimeter Wave Synthesizer Locked to an Optically Transmitted Reference Using Harmonic Mixing”, *Technical Digest of the IEEE Topical Meeting on Microwave Photonics, MWP’97, pp.91-94,* Duisburg, Germany, September 1997.

[19] Attila Hilt, Anne Vilcot, Tibor Berceli, Tamás Marozsák, Béatrice Cabon: “New Carrier Generation Approach for Fiber-Radio Systems to Overcome Chromatic Dispersion Problems”, *IEEE MTT-S Digest, pp.1525-1528,* Baltimore, USA, June 1998.

[20] Attila Hilt: “Transmission et traitement optiques des signaux dans les systèmes de télécommunications hertziens”, *Ph.D. thsesis, Institut National Polytechnique de Grenoble,* Grenoble, France, 17^{th} May 1999.

[21] G.Maury, A.Hilt, B.Cabon, V.Girod, L.Degoud: “Remote Upconversion in Microwave Fiber-Optic Links Employing an Unbalanced Mach-Zehnder Interferometer”, *Proc. of the SPIE’s* 44^{th} *Annual Meeting, Terahertz and Gigahertz Photonics Conference, paper 3795-71,* Denver, Colorado, USA, July 1999.

[22] B.E.A.Saleh, M.C.Teich: “Fundamentals of photonics”, *John Wiley and Sons Inc.,* 1991.

[23] A.Yariv, P.Yev: “Photonics, Optical Electronics in Modern Communications”, 6^{th} edition, *Oxford University Press,* 2007.

[24] Attila Hilt: “Microwave Harmonic Generation in Fiber Optical Links”, *Journal of Telecommunications and Information Technology, pp.22-28, ISSN: 1509-4553,* Poland, 1/2002.

[25] István Frigyes, Attila Hilt, Sándor Csernyin: “Investigations in Microwave Optical Links - Accent on QAM”, *Technical Digest of the International Topical Meeting on Microwave Photonics, MWP’2000, pp.156-159,* Oxford, UK, Sept. 2000.

[26] Attila Hilt, Tibor Berceli, István Frigyes, Eszter Udvary, Tamás Marozsák: “Fiber-Dispersion Compensation Techniques in Optical / Wireless Systems”, *Proc. of MIKON’2002 Conference, Vol.1, pp.25-36,* Gdansk, Poland, 20-22 May 2002.

[27] Mehmet Alp Ilgaz, Eszter Udvary, Bostjan Batagelj: “Influence of Fibre Chromatic Dispersion on the Performance of Analogue Optical Links for an Opto-electronic Oscillator within a 5G Network Structure”, 25^{th} *International Electrotechnical and Computer Science Conference, ERK’2016,* Portorož, Slovenia.

[28] Andreas Stöhr, Ken-ich Kitayama, Toshiaki Kuri: “Chirp Optimized 60 GHz Millimeter-Wave Fiber-Optic Transmission Incorporating EA-Modulator”, *Conference proceedings of ECOC’98, pp.669-670,* Madrid, Spain, 1998.

[29] Jiri Švarný: “Implementation of a precise quadrature point bias controller to the integrated intensity electro-optic modulator”, *Proc. of the* 13^{th} *Biennial Baltic Electronics Conference, BEC’2012, pp.133-136,* Tallin, Estonia, Oct. 2012.

[30] Jiri Švarný: “Bias driver of the Mach-Zehnder intensity electro-optic modulator, based on harmonic analysis”, *Proc. of the International Conference on Mechatronics and Robotics, MEROSTA’2014, pp.184-189,* Santorini, Greece, July 2014.

[31] Tadao Nakazawa: “Low Drive Voltage and Broad-Band $LiNbO_3$ Modulator”, *Technical Digest of the International Topical Meeting on Microwave Photonics, MWP’02, pp.45-48,* Awaji, Japan, November 2002.

[32] Masaharu Doi, Naoki Hashimoto, Tetsu Hasegawa, Takehito Tanaka, Kazuhiro Tanaka: “40 Gb/s Low-drive-voltage $LiNbO_3$ Optical Modulator for DQPSK Modulation Format”, *Conference on Optical Fiber Communication and the National Fiber Optic Engineers Conference, OFC/NFOEC,* March 2007.

[33] John F. Diehl, Vincent J. Urick: “Chromatic Dispersion Induced Second-Order Distortion in Long-Haul Photonic Links”, *Journal of Lightwave Technology, Vol.34, No.20, pp.4646-4651,* 15^{th} October 2016.

ABBREVIATIONS

α	MZM bias, RF part, normalized to V_π
AP	access point
c	speed of light
CD	chromatic dispersion
CPW	co-planar waveguide
CW	continuous wave
D	dispersion parameter (in ps/nm/km)
DC	direct current
DD	direct detection
DFB	distributed feedback (laser)
E/O	electrical-to-optical conversion
E_{opt}	optical field
EPC	evolved packet core
f_{RF}	radio frequency
f_{opt}	optical frequency
GND	ground (electrodes of the optical modulator)
GPON	Gigabit passive optical network
γ	MZM bias, DC part, normalized to V_π
HP	Hewlett-Packard
HP-IB	Hewlett-Packard Interface Bus
IM	intensity modulation
I_{in}	optical intensity at modulator input
I_{opt}	optical intensity (typically mW at MZM output)
I_{out}	optical intensity at modulator output
L	fiber length (usually in km)
LD	laser diode
$LiNbO_3$	Lithium Niobate crystal
λ	wavelength (usually in nm)
μW	microwave (RF signal)
MIMO	multiple-input multiple-output
mmW	millimeter-wave (RF signal)
MZM	Mach-Zehnder modulator
NE	network element
NW	network
O/E	optical-to-electrical conversion
O&M	operation and maintenance
OSSB	single sideband (modulation)
PD	photodiode
P_{f1}	power of the fundamental signal
P_{f2}	power of the second harmonic
P_{f3}	power of the third harmonic
PMD	polarization mode dispersion
RF	radio frequency
R_{PD}	photodiode responsivity (e.g. mA(el.)/mW(opt.))
RoF	radio over fiber (systems)
SCOM	suppressed carrier optical modulation
SMF	single-mode (optical) fiber
SRAN	single radio access network
RRH	remote radio head
V_{DC}	bias voltage of the optical modulator
V_π	half-wave voltage of the modulator at bias port
5G	5^{th} generation mobile NW